



Research article

Internet of Bio Nano Things-based FRET nanocommunications for eHealth

Saied M. Abd El-Atty^{1,*}, Konstantinos A. Lizos², Osama Alfarraj³ and Faird Shawki¹

¹ The Department of Electronics and Electrical Communications Engineering, Faculty of Electronic Engineering, Menoufia University, Menouf 23952, Egypt

² Department of Informatics, Faculty of Mathematics and Natural Sciences, University of Oslo (UiO), Norway

³ Computer Science Department, Community College, King Saud University, Riyadh 11437, Saudi Arabia

* **Correspondence:** Email: sabdelatty@el-eng.menofia.edu.eg.

Abstract: The integration of the Internet of Bio Nano Things (IoBNT) with artificial intelligence (AI) and molecular communications technology is now required to achieve eHealth, specifically in the targeted drug delivery system (TDDS). In this work, we investigate an analytical framework for IoBNT with Forster resonance energy transfer (FRET) nanocommunication to enable intelligent bio nano thing (BNT) machine to accurately deliver therapeutic drug to the diseased cells. The FRET nanocommunication is accomplished by using the well-known pair of fluorescent proteins, EYFP and ECFP. Furthermore, the proposed IoBNT monitors drug transmission by using the quenching process in order to reduce side effects in healthy cells. We investigate the IoBNT framework by driving diffusional rate models in the presence of a quenching process. We evaluate the performance of the proposed framework in terms of the energy transfer efficiency, diffusion-controlled rate and drug loss rate. According to the simulation results, the proposed IoBNT with the intelligent bio nano thing for monitoring the quenching process can significantly achieve high energy transfer efficiency and low drug delivery loss rate, i.e., accurately delivering the desired therapeutic drugs to the diseased cell.

Keywords: Internet of Bio Nano Things (IoBNT); artificial intelligence (AI); forster resonance energy transfer (FRET); nanocommunication; eHealth

1. Introduction

Recently, the Internet of Things (IoT) and biological nano scale technologies have merged to form a promising paradigm, known as the Internet of Bio Nano Things (IoBNT). The IoBNT paradigm, which is based on synthetic biology and nanotechnology, enables the development of a biological embedded computing device, known as bio nano thing (BNT) [1]. Furthermore, these BNTs are intelligent machines that are capable of actuation, sensing, processing, and communication. Therefore, the IoBNT is intended to be a paradigm shift for many related disciplines, such as bio nanosensors-based fluorescence inside intra-body area network (IBAN), and control/manage the interconnection among embedded BNTs via biocyber interface with an external macro network, such as the Internet. In a consequence, various artificial intelligence (AI) algorithms can be used in conjunction with the IoBNT for processing and decision making. As a result, the IoBNT and AI have emerged as promising tools in the field of advanced targeted nanomedicine (ATN), wherein the human body is considered an infrastructure [2]. As a result, IoBNT and AI aid in the design of treatment plans by assisting with drug management or drug discovery.

Additionally, the promising IoBNT paradigm, in conjunction with AI, can be used in ehealth monitoring, detection and diagnostics/treatment of diseases. The term “molecular communications” describes the procedure of encoding/decoding and exchanging data in the form of molecules over short distances [3,4]. The information can be encoded on the concentration, on the frequency and/or on the type of released molecules. Forster Resonance Energy Transfer (FRET) is a well-known type of molecular communication. FRET is a non-radiative energy transfer observed between fluorophore molecules in the 10nm communication range. It should be highlighted that, when compared with other molecular communication systems, FRET is clearly a reliable short-range communication system. The information is encoded in the energy (exciton) transferred between molecules, with no photons or chemical signals emitted. As a result, FRET provides highly reliable communication with fascinating metrics, such as high transmission rates “around 1 Gbit/s,” short transmission delays “around 20 ps,” and low bit error rate “around 10^{-3} ” at the molecular level [3,4].

As a consequence, FRET has discovered numerous successful applications in studying the interaction of medicine nanoparticle drugs with biological systems, such as protein-protein interactions. FRET has recently been used as a biosensor in mechanobiology screening [5,6]. Readers interested in an overview of end-to-end communication-based FRET should refer to [7–10]. Fluorophores, such as fluorescent proteins, quantum dots (QDs) and organic dyes, can be used to label BNTs in the context of preparation nano-systems based on FRET phenomena. Functionalized fluorescent nanodiamonds (FNDs), for example, have recently emerged as superior intracellular thermometry probes with nanometer-scale spatial resolution [11]. Furthermore, under ambient conditions, FND is a highly competitive biomarker and ultrasensitive biosensor. Broad examples of this application, in which medical systems using AI aided in the discovery of the best contents of a multiple types of drugs carried by FNDs for the treatment of human breast cancer are presented in [12]. However, the temperature and magnetic field are defected in diamonds, are key to high-sensitivity bio sensing, as well as may harm the healthy cell that is close to the diseased cell applications [13]. Furthermore, BNTs can be excited by laser/optical, electrical, chemical, or biological energies and then individually relax to the ground state after some time, i.e., excitation lifetime, by fluorescing, i.e., releasing a single photon with a wavelength in their emission spectrum [9]. In terms of drug-target affinity (DTA), the authors [14] have presented an interactive learning mechanism for intramolecular

and intermolecular. The experimental results demonstrated that the probability distribution between the actual and predicted values of DTA can be improved over other methods. On the other hand, the machine learning and convolutional neural network (CNN) for molecular communication in the form of MRI can be embedded in the BNTs, in order to utilize multimodal information in clinical diagnosis and treatment, as proposed in [15]. Furthermore, molecular communications-based FRET can be used in the context of targeted drug delivery systems (TDDS); however, the problem with this model is that continuing to release therapeutic drugs “with high transmission rates around 1 Gbit/s” to diseased cells, may harm healthy cells or cause saturation (congestion) at the RNT. Therefore, we can prevent the potential side effects in TDDS scenario by using FRET quenching processes. There are numerous quenching mechanisms that can prevent the fluorescence of the excited-state donor [16,17]. Quenching can be caused by a number of processes, including FRET, complex formation, collisional quenching and excited state reactions. As a result, quenching is frequently, highly dependent on physical parameters (temperature and pressure), which are included in the diffusion coefficient of the medium. The interaction of a specific, molecular biological target with quenching and dequenching is the basis for activatable optical contrast agents for molecular imaging and high-sensitivity bio sensing applications [18].

Recent advances in small-molecule quenchers used in FRET-based probes in future biomedical applications were presented by the authors [19]. FRET’s progress and promising future are aided by interdisciplinary collaboration in materials science, optical physics, and biomedicine. They proposed developing small-molecule quenchers with broader and deeper quenching regions, as well as improved bioavailability for novel biomedical applications. FRET and BRET-based biosensors are widely used in biological, medical, and environmental research [20]. However, designing FRET and BRET-based biosensors with superior performance for application remains difficult; they presented some solutions, such as determining signal-to-noise ratio, insufficient fluorescence resolution, and photobleaching of reagents. The use of nanomaterials with FP-based biosensors for early-stage diagnosis has been covered by the authors [21]. They came to the conclusion that the size of the fluorescent element affects biosensors. Nanomaterials, which have a high surface area to volume ratio, have the potential to immobilize multiple receptors for multiplexed detection, in addition to reducing the size of the biosensor.

The above recent studies in the field of targeted drug delivery systems have used molecular communication technology to deliver the drug to diseased cells. The Forster Resonance Energy Transfer is one of the most important methods of molecular communication. As a result, the motivation for this work stems from the use of FRET nanocommunication with the quenching process to efficiently deliver therapeutic drugs to diseased cells using intelligent bio nano machines controlled by Internet of Things (IoT) technology. In this work, we make use of FRET quenching phenomenon to enable the IoBNT for monitoring the intermolecular interactions between fluorophore molecules, and, thus, control delivery of the therapeutic drug to the targeted cell. We use the famous pair of fluorescent proteins, EYFP and ECFP, as a pair of the FRET to accomplish the molecular communication. Additionally, we use pulse excitation to control the quenching/dequenching operation by sending a command via biocyber interface to add the effect of intelligent quencher nano thing (Q_{BNT}) in the IBAN. We investigate an analytical framework for IoBNT-based nanocommunication in the presence of fluorescence quenching in order to detect the binding of therapeutic drug “ligand” to the target (diseased) cell “receptor”. We also look into how the concentration of quenchers affects the diffusion-controlled reaction rate. Additionally, we study

the effect of the proposed system parameters in the performance of energy transfer efficiency and the drug loss rate. The contribution of this work can be summarized as follows:

- Proposing a method for integrating IoBNT and AI technologies for TTDS
- Using FRET nanocommunication to accomplish the molecular communications
- Employing the FRET quenching process
- Presenting analytical framework FRET quenching
- Deriving the energy transfer rate and diffusion-controlled reactions
- Providing the quenching concentration to control the transmission rate
- Evaluating the efficiency of drug transmission and drug loss rate with and without the proposed IoBNT.

The rest of this paper is structured as follows: Section 2 describes the FRET principle. Section 3 describes the operational steps of artificial intelligent bio nano things based on the FRET nanocommunication system. Section 4 discusses the different types of quenching processes, and Section 5 describes the proposed system model for the IoBNT and molecular quenching. Section 6 introduces the proposed IoBNT framework based on FRET quenching. Section 7 discusses the numerical results. Section 8 represents the work's conclusion.

2. FRET principles

FRET nanocommunications consists of a nano thing transmitter and a nano thing receiver, which are labeled by fluorescent molecules, that can absorb/emit energy in the visible part of the EM spectrum e.g., light-sensitive proteins and bioluminescent/Fluorescent proteins [22]. For example, two fluorophore molecules are attached to proteins as follows: donor (enhanced yellow fluorescent protein) “EYFP” and acceptor (enhanced cyan fluorescent protein) “ECFP” should be within 10 nm of each other, as shown in Figure 1(a). The emission spectrum, $f_D(\lambda)$ and the absorption spectrum, $\varepsilon_A(\lambda)$ should be significantly overlapped [9]. The critical role in FRET deployment is to ensure sufficient overlap between the $f_D(\lambda)$ spectrum of the D , and the $\varepsilon_A(\lambda)$ spectrum of the A , as shown in Figure 1(b). Energy always takes the form of an energy “exciton”, so we consider that the exciton contains the therapeutic drugs (i.e., nano scale information). Thanks to developments in nanotechnology, it is possible to load therapeutic drugs as nanoparticles (NP) into bio nano thing machines [23]. Therefore, the information is encoded in the energy transfer between fluorophore molecules, with no photons or chemical signals emitted. The rate of energy transfer, $k_T(r)$ from one D to A , is inverse sixth power of the intermolecular distance between them; r . $k_T(r)$ can be solely expressed as [22]:

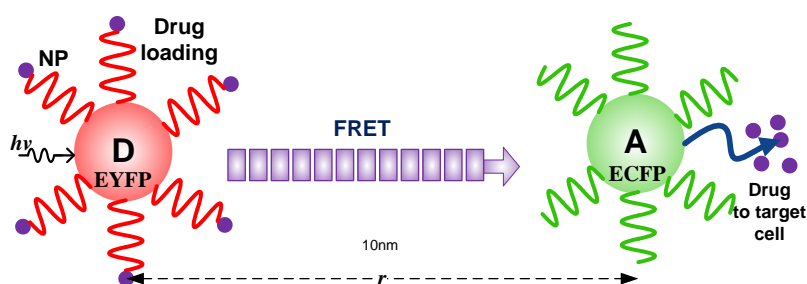
$$k_T(r) = \frac{1}{\tau_D} \left(\frac{R_0}{r} \right)^6 \quad (1)$$

where R_0 denotes the Forster radius, which is defined as the distance at which half of the D 's energy is transferred to the A . τ_D is the decay rate of the D in the absence of an A . Basically, the Forster radius, R_0 , is determined when the rate of energy transfer is equal to the decay rate of the D

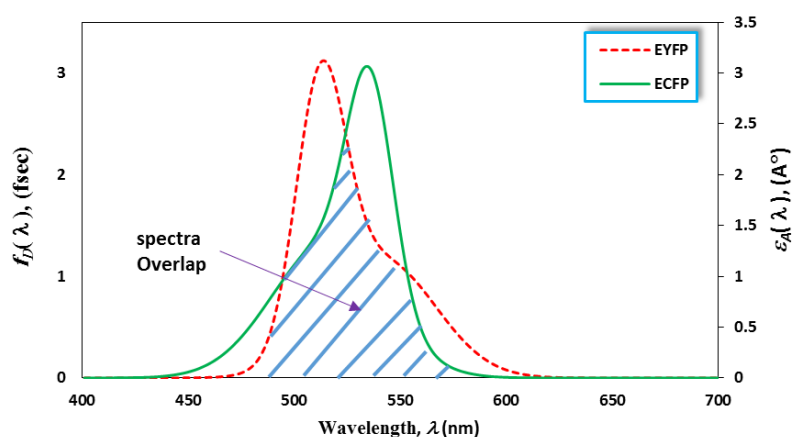
fluorophore. Numerically, the energy “exciton” transfer efficiency η can be computed as follows:

$$\eta(r) = \frac{R_0^6}{R_0^6 + r^6} = \left[1 + \left(\frac{r}{R_0} \right)^6 \right]^{-1} \quad (2)$$

Clearly, efficiency decreases as intermolecular distance, r , increases, and efficiency increases as R_0 increases. On the other hand, fluorescence quenching takes place when the quencher quenched fluorescence emission. The activation of proteins or genes can be determined by fluorescence quenching, wherein the diffusion quencher rate may be added or removed in response to a biological process [24]. Various methods produce quenching as explained in the next section.



(a)



(b)

Figure 1. FRET nanocommunication.

3. Artificial intelligent Bio Nano Thing

Figure 2 depicts the operational steps for AI-based FRET nanocommunication, which is analogous to traditional digital communication. Thanks to emerging nanotechnology and biological science, the development of novel intelligent bio nano thing machines capable of performing all functions of such system, are enabled. As a result, the system’s main components are the transmitter

and receiver bio nano things, which are based on artificial intelligence described as follows [25]: The time-varying response, $x_1(t)$, denotes the source information and source encoder, which allow transmission for stream of binary bits from the intelligent T_{BNT} to R_{BNT} . The time-varying response, $x_2(t)$, is an optical modulator of electrical signal supplied by laser with the wavelength of the emission photon. Actually, this method offers an On-Off Keying (OOK) for modulating laser signal in accordance with the binary data provided by nano component 1. The time-varying response, $x_3(t)$, is the processing of polarization alignment of laser pulses. Then, the microscope step is performed by condensing the signal with a filter, and then transmits it to the nano-communication channel, which is denoted by time-varying response, $x_4(t)$. As a result, the photo detector performs the demodulation process, which is amplified by a low-noise amplifier (LNA). The OOK modulation scheme determines bit “1” if the received signal is greater than a threshold level; otherwise, bit “0”. The output binary sequence of the demodulated signal is serially passed to the destination for source decoding using the nano-units $x_1(t)$ to $x_4(t)$.

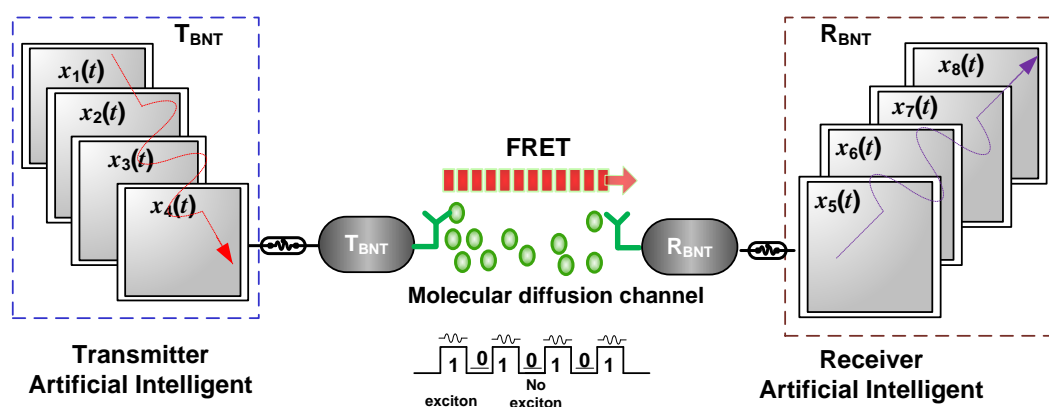


Figure 2. Block diagram of AI-FRET Nanocommunications.

Instead of requiring an extensive clinical data set for AI analysis and training in order to provide accurate diagnosis and prognosis, the proposed model relies on signals acquired from Bio nano thing-based AI technology, which serve as sensors, sending electrical and biological signals via a biocyber interface [26,27]. These sensors aid in detecting biological changes in the IBAN (diseased site), and sending it to Internet via the biocyber interface. The accuracy of such a model is determined by the goodness of fit between the experimental and predicted curves. As a consequence, various AI algorithms can be used in conjunction with the IoBNT for processing and decision making in the prediction of biological signal process [28], and an example of such algorithm is illustrated in Figure 3. The objective of AI is to use a smart decision making system to assist the IoBNT in monitoring the drug delivery to the target cell. The bio nano thing-based AI system here is a highly effective tool for calculating the efficiency of energy transfer between two fluorophores, whether in ensembles or attached to individual molecules, where fluorophores can be distributed uniformly or randomly on the surface of R_{BNT} . It is challenging to describe, assuming that the fluorophores' diffusion rate is much slower than their transfer rate. In order to calculate FRET between constrained fluorophores, we characterise the T_{BNT} “donor” intensity decay and quantum yield for fluorophores. From there, we calculate transfer efficiencies directly from the proportion of absorbed photons that are transferred to R_{BNT} “acceptors”.

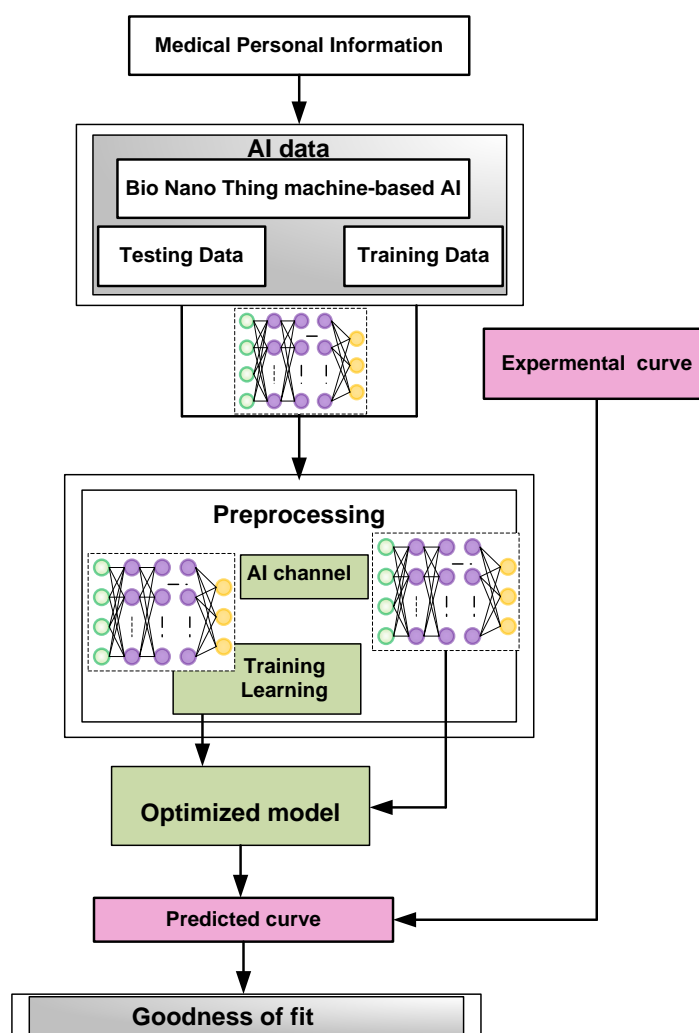


Figure 3. Illustration example of an AI for detecting bio signal.

4. Quenching types

Fluorescence quenching takes place when the quencher quenched fluorescence emission. Subsequently, quenching depends usually on environmental and intrinsic conditions, such as pressure and temperature, and there are many types of chemical quenchers such as molecular oxygen, iodide ions and acrylamide [29–31]. The activation of proteins or genes can be determined by fluorescence quenching wherein the quencher may be added or removed in response to biological actions. Various methods produce quenching, such as collisional quenching, fluorescence resonance energy transfer, complex-formation and excited state reactions. We illustrated in Figure 4 the mechanism of different quenching methods. The FRET quenchers function as FRET acceptors; they are able to accept energy in a similar manner, but they return to the ground state from the excited state via non-radiative decay pathways rather than by emitting light. Quenchers have a high extinction coefficient and a broad absorption spectrum [29]. The intercellular signaling in living cells, based on protein-protein interplay, is studied by computing the FRET sensitized-quenching transition factor (G factor) and optical system in a particular structure of 3-cube FRET [30].

When a fluorophore forms a complex with a quenching molecule before being excited, this process is known as contact quenching. Because the fluorophore is in direct contact with the quenching molecule, the energy from the excitation is immediately transferred to the contact molecule, where it is then lost as heat. Collisional quenching happens when an excited fluorophore reacts with a quencher molecule in solution, which right away results in the energy being transferred to the contact molecule, and the excited fluorophore relaxing [31]. The collisional or dynamic quenching mechanism is considered as one of the bimolecular interactions between fluorophores and quenchers, which results in reducing the fluorescence emission (or intensity), as well as a lifetime of excited state. In this mechanism, the quencher (such as oxygen, which is one of the well-known collisional quenchers) diffuses in aqueous medium and then collides with the excited fluorophore molecule during its lifetime. As long as the collision happens between the quencher and fluorophore molecule, the fluorophore goes back to the ground state without emitting a photon. This phenomenon of collisional quenching is experienced in distance and time expansion medium provided by fluorescence lifetime. The diffusive distance of oxygen quencher during the lifetime of the excited state (τ_a) is expressed by $\Delta x^2 = 2D \tau_a$, where D is the diffusion coefficient of the quencher. For instant, when an oxygen quencher with $D = 2.5 \times 10^{-5} \text{ cm}^2/\text{sec}$ in water medium at 25°C , there will be 7 nm or 70 \AA movement within 10 ns, which is comparable to the diameter of protein. In the case of rapid-diffusion limit, some fluorophores have lifetimes reach 400 ns, and, hence, the diffusion of oxygen quencher can be observed at distance over 45 nm or 450 \AA , thereby, with employing longer-lived probes with micro second lifetimes, the diffusion over larger distance is still observed [32]. To lessen fluorescence bleed-through between the donor and acceptor, FRET quenchers have been developed. FRET quenchers function as FRET acceptors in a manner similar to that of conventional FRET-based fluorophores; they are capable of accepting energy, but unlike conventional FRET-based fluorophores, they do not emit light upon returning from the excited state to the ground state [32].

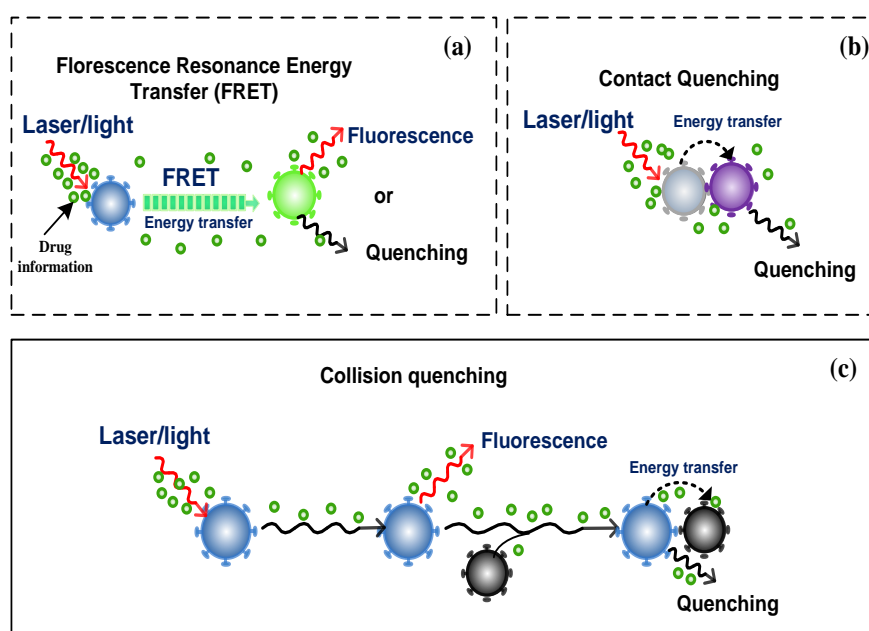


Figure 4. Types of molecular quenching.

In a similar way of [32], we consider there are multiple quenchers in the medium; therefore, we can apply a natural modification of the Eq (2), which accounts for multiple quenchers as follows:

$$\eta_q(r_q, n) = \frac{n_q R_0^6}{n_q R_0^6 + r_q^6} \quad (3)$$

where n_q is the mean number of quenchers. This accounts for multiple energy transfer channels (each having the same transfer rate) between the donor and closer quencher (Q). We can rearrange the above Eq (3) to obtain the required distance of quencher position as follows:

$$r_q = R_0 \left[\frac{n_q(1-\eta_q(r_q, n_q))}{\eta_q(r_q, n_q)} \right]^{1/6} \quad (4)$$

Equation (4) refers to the position distance of a quencher that can be monitored via IoBNT, in order to control/manage the transmission of therapeutic drugs.

5. System model

We consider a scenario of a molecular communications system with AI bio nano thing working by fluorescent to perform FRET communication inside a human intra-body area nanonetwork (IBAN). We envision that the system is controlled by the IoBNT paradigm, as illustrated in Figure 5. The main element in the IoBNT paradigm is the biocyber interface, which converts an electromagnetic (EM) signal into a biological signal or vice versa, as described in [33]. As a consequence, the biocyber interface is considered as the seamless interconnection of different technologies in diverse application environments “human body and medical personnel through Internet”. The emerging biocyber interface in [34] can be used in the proposed system model. Furthermore, the estimation of the biocyber with CNN for the IoBNT can be computed as presented in [35], and the privacy and security of the IoBNT-based biocyber interfaces is introduced in [36].

The IBAN can be strategically implanted near the diseased site using nanotechnology tools [22]. The proposed IBAN is made up of three intelligent bio nano thing machines: T_{BNT} , Q_{BNT} and R_{BNT} , which stand for transmitter, quencher, and receiver, respectively. All BNTs are considered bionanosensors-based fluorescence, and have the capacity to convert signals into different formats, including accepting photons, interacting via FRET and releasing electrons. In other words, the aim of the bio nano things machine is to collect sensory information from outside/inside the Internet/human body via the biocyber interface. Furthermore, the incorporation of bio nano thing machines with AI will enable real-time monitoring for any non-linearity in the biosensor response under unavoidable internal conditions or infection [21,22]. The proposed system's complete design is beyond the scope of this paper. However, some recent studies that investigated the enabling technology, which performed the injection of nano thing machine inside the human body and detection of specific molecules across the diseased cell [3]. According to FRET phenomena, the three bio nano thing machines are envisioned in the proposed targeted drug delivery system, based on fluorophore labeled ligand, and FRET quencher is used to reduce side effects in healthy cells.

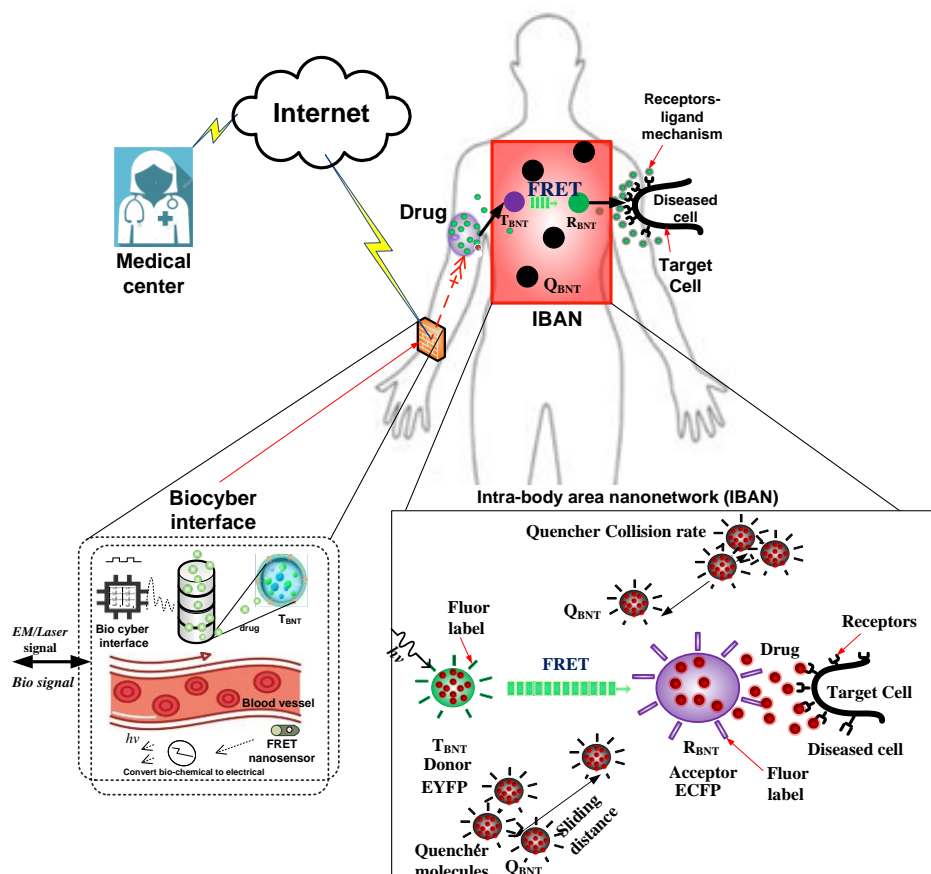


Figure 5. Proposed IoBNT paradigm-based AI with FRET nanocommunication.

As a result, the main elements of the proposed system are the transmitter nano thing, T_{BNT} , i.e., the donor, and the acceptor is the receiver bio nano thing, R_{BNT} , with the ability of IoBNT technology to add or remove the effect of the quencher bio nano thing, Q_{BNT} . The T_{BNT} is equipped with a light sensitive molecule (i.e., fluorophore), in order to adjust the bio-molecular activities when illuminated with light/laser of different wavelengths (λ) via the biocyber interface. The FRET discipline states that, when the T_{BNT} receives light, it releases the drug molecules in the form of energy “exciton” information, which propagates and is eventually received by R_{BNT} (i.e., diseased cell). The IoBNT controls the quenching/dequenching operation by sending a command via biocyber interface to add the effect of the quencher nano thing (Q_{BNT}) in IBAN, and thus Q_{BNT} receives the overwhelm drug transmission instead of R_{BNT} , preventing an overflow of drug transmission at R_{BNT} that may harm healthy cells.

6. Proposed framework of IoBNT-based FRET quenching

The IoBNT is a cutting-edge paradigm for managing embedded computing of biological nano things in various nanomedical applications that originates from synthetic biology and advancements in nanotechnology [1,9]. The need for biological nanomachines to communicate with one another based on the transfer of information via the Internet gave rise to the idea of IoBNT [37]. The proposed IoBNT aims to control and manage the bio nano thing machines in the implanted IBAN, in

order to precisely deliver the desired therapeutic drugs to the diseased cell. Further, quenching reduces the side effects in the healthy cell, as shown schematically in Figure 6. After labelling the fluorophores and attaching them to the bio nano thing machines, T_{BNT} , Q_{BNT} , and R_{BNT} . The IoBNT monitors the configurations and positions of Q_{BNT} and R_{BNT} . According to the FRET principle, the energy or exciton transfer rate, the IoBNT, computes the distance between the bio nano thing machines and allows the exciton transfer.

As a result, the availability of receptors on the surface of R_{BNT} is calculated. The rate of exciton transfer, $k(t)$, is then calculated. The IoBNT manages and controls drug delivery to the diseased cell by monitoring drug overflow at the R_{BNT} . If there is overflow, the IoBNT activates the quenching process by adding Q_{BNT} effects, becoming the acceptor and, thus, receiving the drug instead of R_{BNT} . This mechanism avoids side effects, and, thus, the drug delivery efficiency is estimated using FRET efficiency. In the proposed model, the goal of IoBNT is to manage/control the function of the quencher nano thing (Q_{BNT}) machine. It is difficult to describe because it is assumed that the fluorophores' diffusion rate is much slower than their transfer rate. As a result, we should be able to determine the time-dependent rate constant of Q_{BNT} in the medium of the implanted IBAN. Typically, quenching is determined by the environment and intrinsic conditions in terms of the diffusion coefficient of the medium.

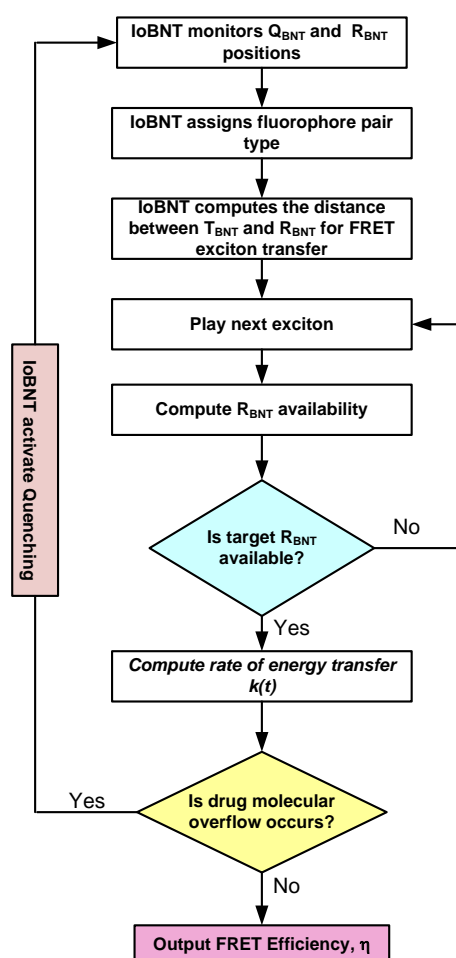


Figure 6. Proposed IoBNT paradigm-based FRET nanocommunication.

Furthermore, the possibility of quenching is highly sensitive to molecular factors and distance, which affect the energy transfer rate and the likelihood of contact. These factors produce transient effects, causing the decay of T_{BNT} emission (or intensity) to be non-exponential. To calculate the quencher concentration, we use well-known models, such as the Smoluchowski and radiation boundary condition (RBC) models [31]. The Smoluchowski model has solved Fick's second law for the quenching phenomenon in medium between two nano things machines, the quencher (Q_{BNT}) and transmitter (T_{BNT}). The deduced concentration of the diffusion quenchers, $C_q(r, t)$ (in molecules/cm³) is given by [31]:

$$C_q(r_q, t) = C_0 \left[1 - \frac{R_s}{r_q} \operatorname{erfc} \left(\frac{r_q - R_s}{\sqrt{4D_s t}} \right) \right] \quad (5)$$

where, C_0 is the initial concentration of the diffusion quenchers, and r_q is the distance from origin to the quencher. D_s denote the sum of diffusion coefficients of the Q_{BNT} and T_{BNT} machines. R_s is always taken as the sum of the radii of two molecules. It is informative to consider the concentration according to the distance and the size of the quencher. Intuitively, it is necessary to study the fluorescence phenomenon in the present quenching by investigating the interaction between Q_{BNT} and T_{BNT} machines in close proximity. According to the bimolecular interactions between the electron clouds of the two molecules, Q_{BNT} and T_{BNT} machines, the mean flux (ϕ) at time t in a sphere of radius R_s can be derived as follows:

$$\phi = 4\pi(R_s)^2 D_s \frac{\partial C_q(r_q, t)}{\partial r} \Big|_{r=R_s} = 4\pi R_s D_s C_0 \left[1 + \frac{R_s}{\sqrt{\pi D_s t}} \right] \quad (6)$$

In reality, the diffusional rate constant is time-dependent, $k(t)$, which is known by Smoluchowski diffusion-controlled reactions, and can be given by

$$k(t) = \frac{\phi}{C_0} = 4\pi R_s D_s N_A \left[1 + \frac{R_s}{\sqrt{\pi D_s t}} \right] \quad (\text{in L mol}^{-1} \text{sec}^{-1}) \quad (7)$$

In Eq (7), C_0 with unit moles per liter and N_A is Avogadro's number per mole. D_s in (cm².sec⁻¹) and R_s in (cm). However, the authors in [30] reported that the probability of every quencher may not collide with fluorophore molecules at distance R_s from the origin. They derived a more realistic expression of the flux, as follows:

$$\phi = \kappa_q \times [4\pi R_s^2 C_q(R_s, t)] \quad (8)$$

where, κ_q (in cm.sec⁻¹) is the bimolecular quenching constant that measures the efficiency of the collisional quenching. The concentration of quencher in Eq (8) refers to the RBC model; the flux can be given by [31]

$$\phi = \frac{4\pi D_s R_s C_0}{1 + D_s/R_s \kappa_q} \left[1 + \frac{R_s \kappa_q}{D_s} e^{x^2} \operatorname{erfc}(x) \right] \quad (9)$$

where, $x = \frac{\sqrt{D_s t}}{R_s} \left[1 + \frac{R_s \kappa_q}{D_s} \right]$

Equation (9) can be exemplified by asymptotic expression of $\operatorname{erfc}(x)$ as follows:

$$\phi = 4\pi\dot{R}_s D_s C_0 \left[1 + \frac{\dot{R}_s}{\sqrt{\pi D_s t}} \right] \quad (10)$$

where, $\dot{R}_s = \frac{R_s}{1 + D_s/R_s \kappa_q}$

Therefore, we can obtain the time-dependent rate constant, $k(t)$, as in Eq (11) by exchanging the parameter R_s by (\dot{R}_s) as follows:

$$k(t) = 4\pi\dot{R}_s D_s N_A \left[1 + \frac{\dot{R}_s}{\sqrt{\pi D_s t}} \right] \quad (11)$$

7. Numerical results

In this section, we analyze the performance evaluation of the proposed IoBNT with bio nano thing using FRET nanocommunication in terms of energy transfer efficiency in the presence of the quenching concentration. We used EYFP and ECFP as the FRET pair to accomplish the nanocommunication between T_{BNT} , and R_{BNT} while the fluorescent is attached to intelligent Q_{BNT} . In the implanted IBAN, the position of nano machines (T_{BNT} , R_{BNT} and Q_{BNT}) are randomly distributed, and increment at each time step according to the normal distribution $N(0, \sqrt{2D\Delta t})$ [38]. We assumed the On-Off Keying (OOK) modulation scheme by encoding 1-bit information into the presence or absence of a single exciton. We consider that the Forster distance, R_0 , is changed from 1-5nm, and the diffusion coefficient range is changed from 10^{-5} to 10^{-7} cm²/s, depending on the molecule type. We conduct the Monte Carlo technique in order to simulate the drug transmission in the molecular channel by varying the concentration [39]. Assuming that an exciton realizes only one activity, such as FRET or fluorescence, during a simulation time step, the simulations are carried out in MATLAB by breaking down the entire process into small time intervals.

Then, we performed extensive simulations to compute the impact of the system parameters on the proposed IoBNT with the intelligent bio nano thing machines and FRET nanocommunication, as described in the next subsections. We assumed that the waveform of the laser excitation composed of very short pluses (its range from pico to nano second) which comparable with the lifetimes of the florescent molecules, and therefore, we consider the excitation period, τ_H , between two successive pluses should be greater than the maximum of the lifetime of T_{BNT} and Q_{BNT} as follows: $\tau_H = \max\{\tau_D, \tau_Q\}$, where τ_Q is the excited lifetime of Q_{BNT} . As we mentioned in the proposed system model, the pair of FRET communication is ECFP-EYFP, and their lifetime is approximately 2.68 and 2.88 ns [40]. As a consequence, the excitation of the T_{BNT} by the laser source at the starting moment, τ_H , relates to bit 1, otherwise bit 0 at no excitation.

7.1. Impact of quenching in IoBNT

Figure 7 shows the concentration of the diffusion quenchers with varying time, t , for different distance, r_q . As we can see the concentration of quenching, C_q decreases as the time increases for all curves. On the other hand, when the separation distance between Q_{BNT} and T_{BNT} machines is large, C_q decreases rapidly. Intuitively, it is necessary to study the fluorescence phenomenon in the presence of quenching by investigating the interaction between Q_{BNT} and T_{BNT} machines in close

proximity. Additionally, this plot will make the decision of IoBNT to monitor the locations of quencher and its concentration.

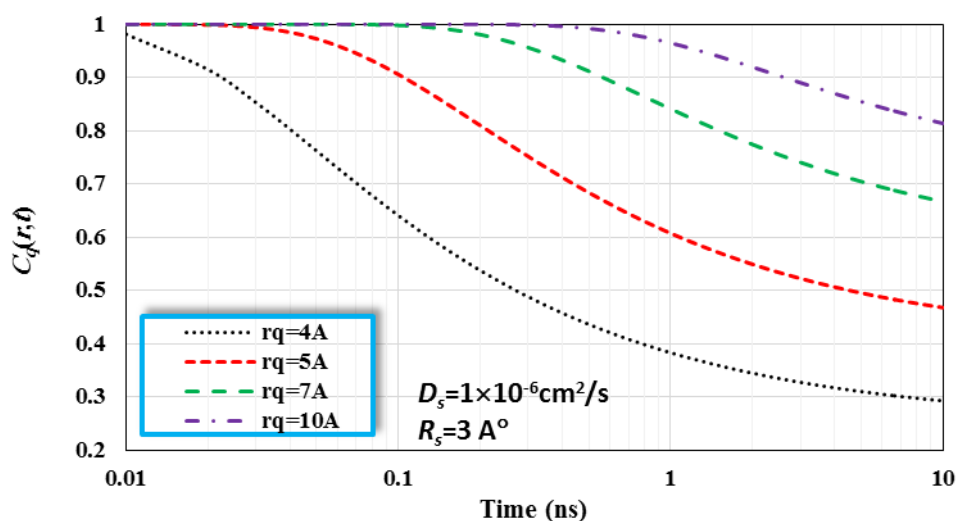


Figure 7. $C_q(r, t)$ versus t with varying separation distance r_q .

As mentioned previously, the quencher inside the proposed intra body area nanonetwork (IBAN) is influenced by the pressure and temperature that included in the form of the diffusion of nano things machine in the medium. Wherein $D_s = k_B T / 6\pi\sigma R_s$, where k_B is Boltzmann's constant, σ is the medium viscosity at the temperature, T , in kelvin, and R_s is the molecular radius. Additionally, the efficiency of quenching can be computed from the observed value of k_q , if the diffusion coefficients and molecular radii are known. Subsequently, we compute the diffusion rate according to Smoluchowski and RBC models. In Figure 8, we plot the diffusion-controlled reaction rate constant, $k(t)$, for the Smoluchowski and RBC models to compare the two theoretical models. The medium's characteristic is indicated within the plot. The main distinction between the Smoluchowski and RBC models is the point of contact. The fluorophore molecule is rapidly deactivated upon contact with the quencher in Smoluchowski, resulting in an infinite quencher concentration gradient around the fluorophore. When T_{BNT} and Q_{BNT} come into contact, the quenching concentration occurs at a finite rate constant, k_q . As we can see for both models, the value of $k(t)$ decreases as the time increases from nano second (ns) range to pico second (ps) range. On the other hand, we observe that, the value of $k(t)$ for RBC model is high at short times over 1 ns compared to the predicted value of k_q , while for Smoluchowski model the value of $k(t)$ diverges to infinity at short times. This is due to the rapid quenching of closely distant T_{BNT} and Q_{BNT} pairs. Additionally, the transient effects are approximately complete at 10 ps and do not exist at 1 ns.

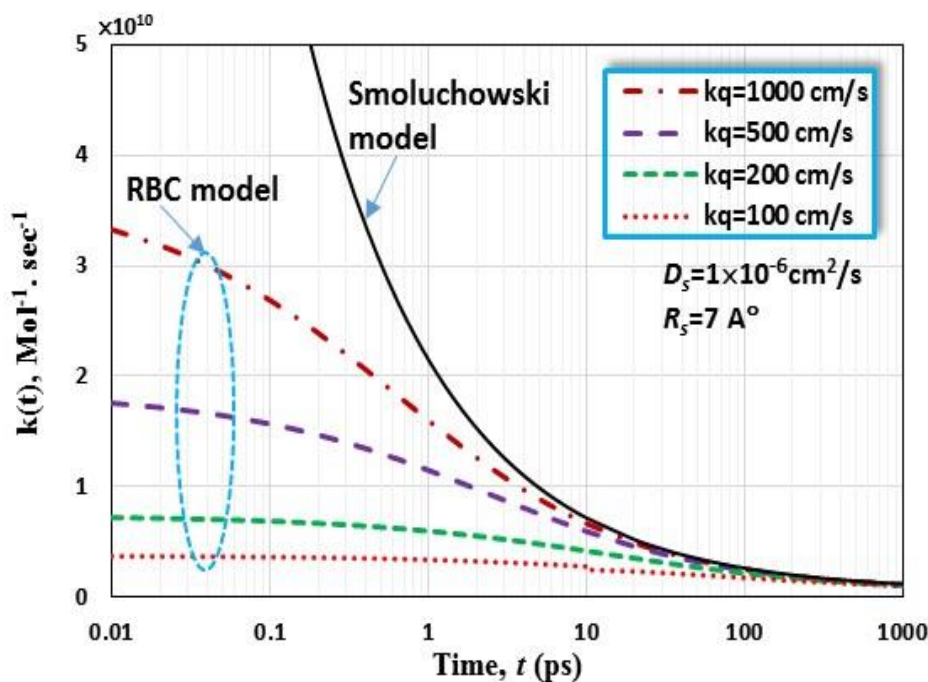


Figure 8. $k(t)$ versus t for Smoluchowski and RBC model.

The efficiency of the quenchers as a function of the separation distance between the T_{BNT} and Q_{BNT} is shown in Figure 9, while the number of quenchers, n_q , is varied. In reality, we have calculated the likelihood of finding n_q quencher in the volume of IBAN using the Poisson distribution as shown below:

$$P(n_q) = \frac{\mu^{n_q}}{n_q!} e^{-\mu} \quad (12)$$

where μ is the mean number of quencher bio nano thing-based AI in the implanted IBAN. In order to deliver the desired therapeutic drug to the target cell, the IoBNT, therefore, keeps track of the quantity of quenchers, n_q , in the IBAN. Evidently, based on Eq (12), the IoBNT determines the likelihood that no quencher is close to the IBAN as

$$P(0) = e^{-\mu} \quad (13)$$

As we can see in Figure 9, the efficiency of the quenching is very high when the distance between T_{BNT} and Q_{BNT} is very small, and then decreases dramatically by increasing the intermolecular distance to approach zero. On the other hand, the influence of the number of the quencher, n_q has significantly affected the performance of the quenching process. Obviously, when, n_q , is small, the efficiency of quenching is low compared with the large number of n_q , because of increasing the number of quenchers i.e., increasing the quenching concentration results in ensuring the quenching process by receiving all the drugs transmitted from T_{BNT} before reaching the R_{BNT} . We validate this observation, by plotting the transfer energy rate versus quencher distance with varying the number of quenchers, n_q , as depicted in Figure 10. As we can see, the energy transfer rate decreases with increasing the distance. However when the number of quenchers is high, the energy transfer rate is kept at high level.

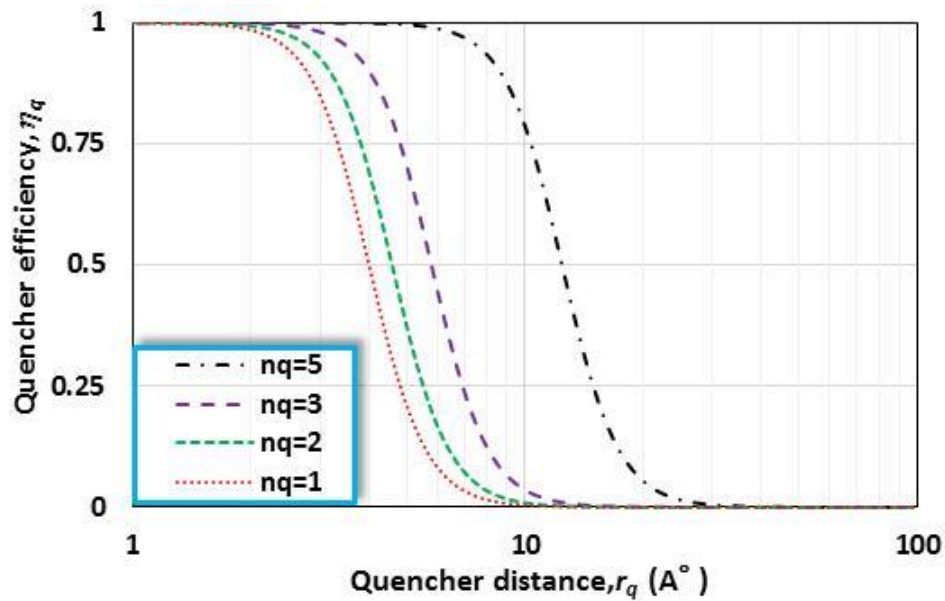


Figure 9. Quenching efficiency versus distance with varying n_q .

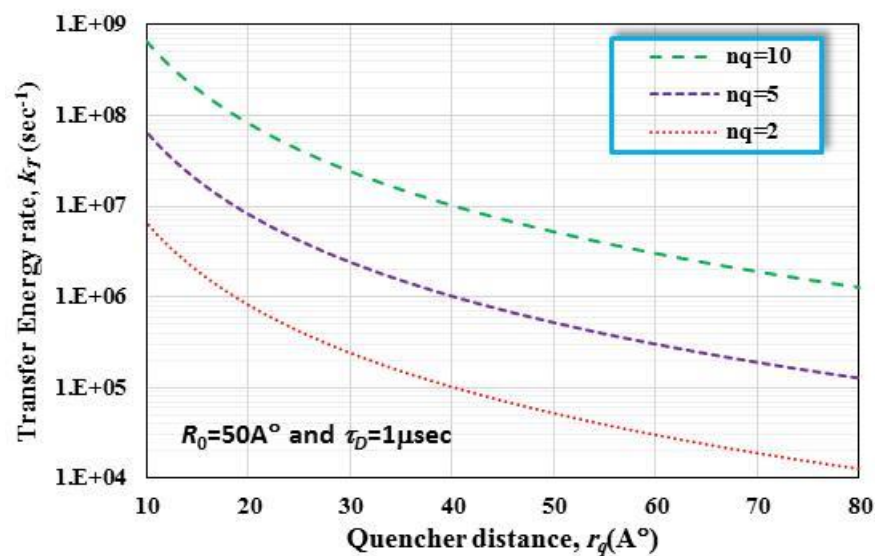


Figure 10. Energy transfer rate versus distance with varying n_q .

7.2. Impact of diffusion coefficient in IoBNT

According to the observed results in the above subsection, we study the performance of energy transfer efficiency in terms of diffusion coefficient, as illustrated in Figure 11. The figure shows the Forester efficiency as a function of sum diffusion coefficient, D_s , for different values of Forester distance (R_0) when the lifetime of florescent attached to T_{BNT} is $\tau_D = 1\mu\text{sec}$. Generally, the efficiency of energy transfer increases as diffusion coefficient increases. Obviously, when the value of R_0 is large, the efficiency of energy transfer increases significantly. We repeated the same simulation results but with changing the lifetime of florescent attached to T_{BNT} . We run this simulation at $R_0 = 5$

nm and for three values of $\tau_D = 1\text{msec}$, $1\mu\text{sec}$ and 1nsec depicted in Figure 12. Obviously, it is better to use fluorescence with a small lifetime to guarantee high efficiency of energy transfer. We also observe when $\tau_D = 1\text{sec}$, the efficiency of energy transfer is high when the diffusion coefficient is small; however it vanishes when diffusion coefficient is high.

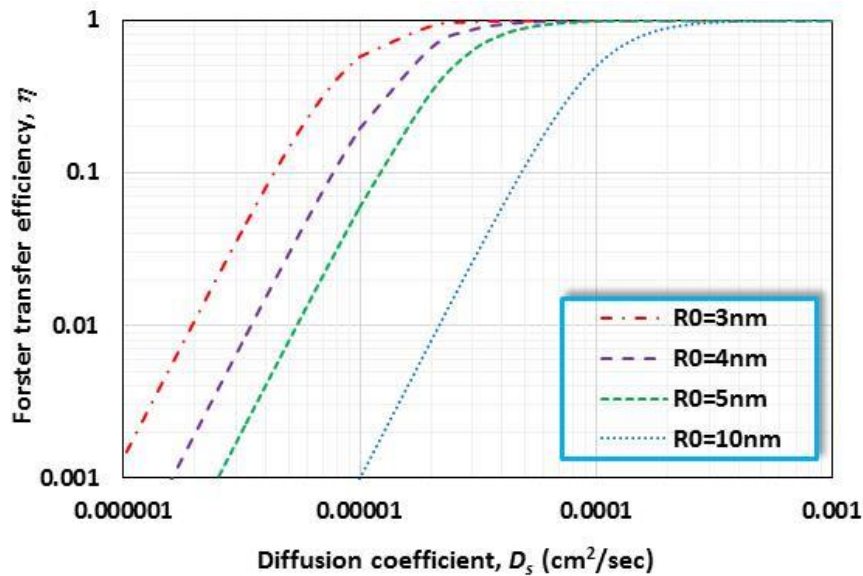


Figure 11. Energy transfer efficiency versus diffusion coefficient with varying R_0 .

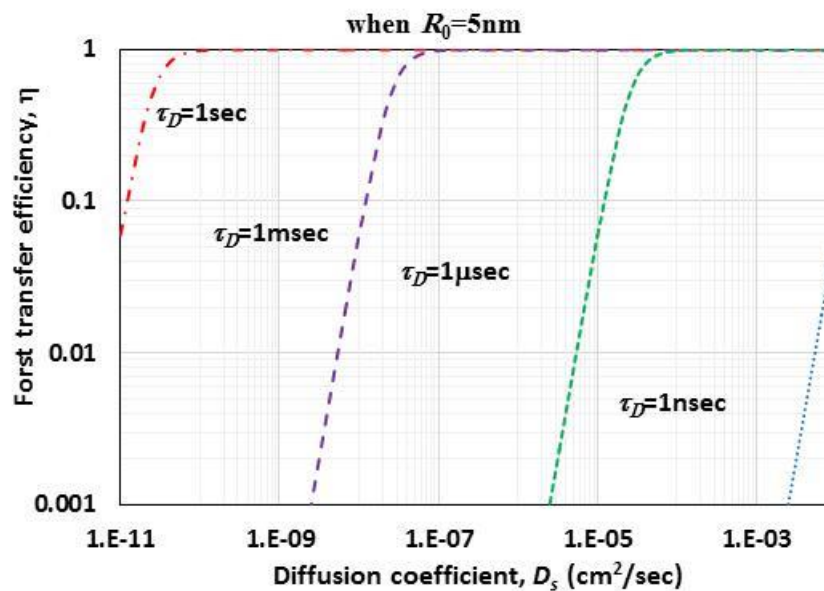


Figure 12. Energy transfer efficiency versus diffusion coefficient with varying τ_D .

7.3. Performance comparison with and without proposed IoBNT

Figure 13 shows the simulation results of the efficiency of energy transfer versus the transmission rate of sending the therapeutic drugs via IoBNT with varying the number of the

quenchers inside the implanted IBAN. Here, we consider the transmission rate, the amount of drug concentration per unit time. In other words, every time step or slot in the interval of excitation shows that T_{BNT} is sending amounts of drug concentration, i.e., refers to the transmission rate. Generally, we can observe that the efficiency of energy transfer reaches to peak point at the starting of the transmission, and, thus, reduces dramatically when the transmission rate increased. In fact, this plot or outcome refers to the channel impulse response of the proposed system. Additionally, it is clear that when the number of quenchers is high, the IoBNT can guarantee the high efficiency of energy transfer in comparison with the small number of quenchers.

Figure 14 shows the simulation and analytical results of the efficiency of energy transfer versus the intermolecular separation distance, r , between T_{BNT} and R_{BNT} in the case of employing proposed IoBNT and without employing it. As we can observe, the efficiency of energy transfer of the two cases are the same when the separation distance between T_{BNT} and R_{BNT} is small. However, when the separation distance between T_{BNT} and R_{BNT} increases, the case with the proposed IoBNT is superior. This is because the presence of a quencher nano machine allows the IoBNT to monitor the diseased cell, and, thus, control the drug transmission rate. For example, if the intermolecular separation distance between T_{BNT} and R_{BNT} is 8nm, the efficiency gain is approximately 12%.

Figure 15 depicts the drug lost rate versus the excitation period with and without the proposed IoBNT. The drug lost rate is defined as the ratio of the drug absorbed by the Q_{BNT} to the total amount of drug concentration transmitted by the T_{BNT} during the excitation period. It is the amount of data that the destination cannot receive during the transmission period or the amount of data that overflows at the destination, according to network theory. This mechanism protects healthy cells from damage, thereby reducing side effects. For example, at a 100ns excitation time, the improved percent of drug loss rate is about 15.5%.

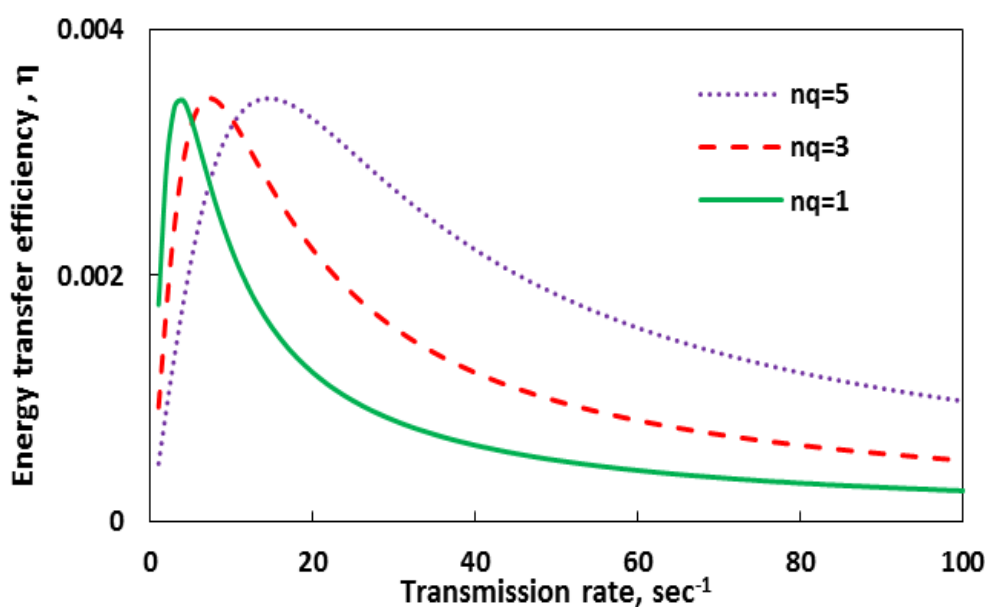


Figure 13. Energy transfer efficiency versus transmission rate with varying n_q .

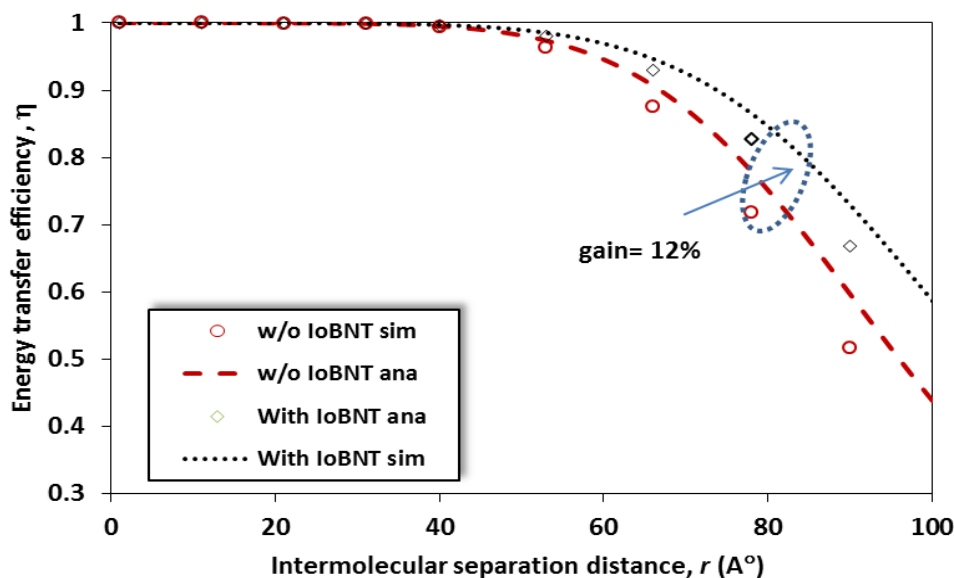


Figure 14. Performance comparison of efficiency with and w/o proposed IoBNT.

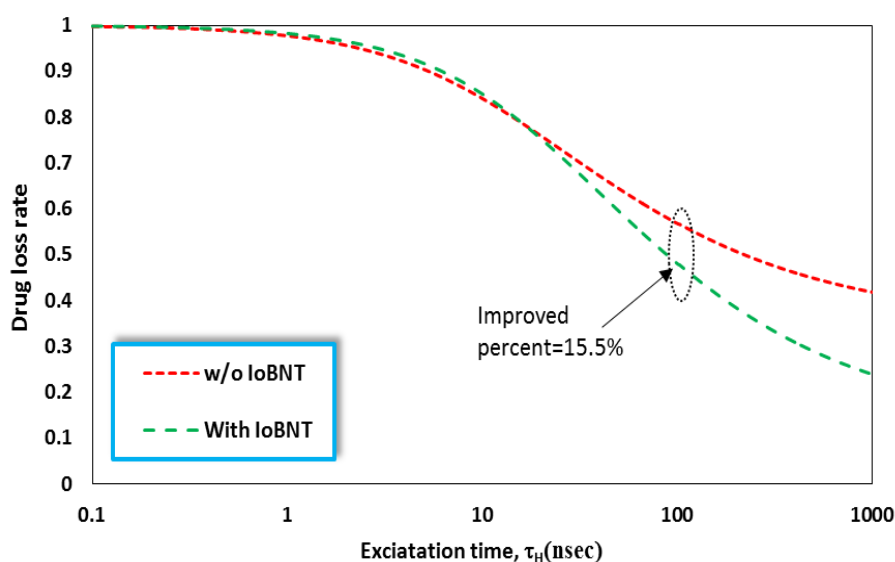


Figure 15. Drug loss rate with and w/o the proposed IoBNT.

8. Conclusions

An analytical framework for IoBNT that enabled the interconnection of group intelligent bio nano thing via FRET nanocommunications in the presence of quenching, in order to deliver a therapeutic drug to the targeted cell, is presented in this paper. The aim of the proposed IoBNT is to monitor the delivery of drugs to the diseased cell by using the quenching process to avoid the side effects. The effect of diffusion quencher concentration on energy transfer efficiency performance was investigated. The numerical results revealed that, in order to realize sophisticated applications of bio nano things in promising targeted drug delivery systems via IoBNT, quenching concentration and diffusion-controlled reaction rate must be considered. Further investigation of the drug transmission

in the IoBNT environment, as well as studying the diffusion of drug to the membrane of the cell, will be our future work.

Acknowledgments

This work was funded by the Researchers Supporting Project number (RSP2023R102), King Saud University, Riyadh, Saudi Arabia.

Conflict of interest

The authors declare that they have no conflicts of interest to report regarding the present study.

References

1. M. Kuscu, B. D. Unluturk, Internet of Bio-Nano Things: A review of applications, enabling technologies and key challenges, *ITU J. Future Evol. Technol.*, **2** (2021), 1–24. <https://doi.org/10.52953/CHBB9821>
2. P. Manickam, S. A. Mariappan, S. M. Murugesan, S. Hansda, A. Kaushik, R. Shinde, et al., Artificial Intelligence (AI) and Internet of Medical Things (IoMT) assisted biomedical systems for intelligent healthcare, *Biosensors*, **12** (2022), 1–29. <https://doi.org/10.3390/bios12080562>
3. I. F. Akyildiz, F. Brunetti, C. Blazquez, Nanonetworks: A new communication paradigm, *Comput. Networks*, **52** (2008), 2260–2279. <https://doi.org/10.1016/j.comnet.2008.04.001>
4. T. Nakano, T. Suda, M. Moore, R. Egashira, A. Enomoto, K. Arima, Molecular communication for nanomachines using intercellular calcium signaling, in *5th IEEE Conference on Nanotechnology*, (2005), 1–5. <https://doi.org/10.1109/NANO.2005.1500804>
5. D. M. Charron, G. Zheng, Nanomedicine development guided by FRET imaging, *Nano Today*, **18** (2018), 124–136. <https://doi.org/10.1016/j.nantod.2017.12.006>
6. P. Kulakowski, K. Turbic, L. M. Correia, From nano-communications to body area networks: A perspective on truly personal communications, *IEEE Access*, **8** (2020), 159839–159853. <https://doi.org/10.1109/ACCESS.2020.3015825>
7. H. Chen, H. L. Puhl, S. V. Koushik, S. S. Vogel, S. R. Ikeda, Measurement of FRET efficiency and ratio of donor to acceptor concentration in living cells, *Biophysics*, **91** (2006), 39–41. <https://doi.org/10.1529/biophysj.106.088773>
8. L. Liu, F. He, Y. Yu, Y. Wang, Application of FRET biosensors in mechanobiology and mechanopharmacological screening, *Front. Bioeng. Biotechnol.*, **8** (2020), 1–17. <https://doi.org/10.3389/fbioe.2020.595497>
9. M. Kuscu, O. B. Akan, The Internet of molecular things based on FRET, *IEEE Internet of Thin. J.*, **3** (2016), 4–17. <https://doi.org/10.1109/JIOT.2015.2439045>
10. M. Kuscu, O. B. Akan, A physical channel model and analysis for nanoscale molecular communications with Förster resonance energy transfer (FRET), *IEEE Trans., Nanotechnol.*, **11** (2012), 200–207. <https://doi.org/10.1109/TNANO.2011.2170705>
11. S. A. Qureshi, W. W. W. Hsiao, L. Hussain, H. Aman, T. N. Le, M. Rafique, Development of fluorescent nanodiamonds for optical biosensing and disease diagnosis, *Biosensors*, **12** (2022), 1181 <https://doi.org/10.3390/bios12121181>

12. Z. H. Chen, L. Lin, C. F. Wu, C. F. Li, R. H. Xu, Y. Sun, Artificial intelligence for assisting cancer diagnosis and treatment in the era of precision medicine, *Cancer Commun. (Lond)*, **41** (2021), 1100–1115. <https://doi.org/10.1002/cac2.12215>
13. Y. Tian, A. C. Nusantara, T. Hamoh, A. Mzyk, X. Tian, F. Perona, et al., Functionalized fluorescent nanodiamonds for simultaneous drug delivery and quantum sensing in HeLa cells, *ACS Appl. Mater. Interfaces*, **14** (2022), 39265–39273. <https://doi.org/10.1021/acsami.2c11688>
14. Z. Zhu, Z. Yao, G. Qi, N. Mazur, B. Cong, Associative learning mechanism for drug-target interaction prediction, preprint, arXiv:2205.15364. <https://doi.org/10.48550/arXiv.2205.15364>
15. Z. Zhu, X. He, G. Qi, Y. Li, B. Cong, Y. Liu, Brain tumor segmentation based on the fusion of deep semantics and edge information in multimodal MRI, *Inf. Fusion*, **91** (2023), 376–387. <https://doi.org/10.1016/j.inffus.2022.10.022>.
16. X. Peng, D. R. Draney, W. M. Volcheck, Quenched near-infrared fluorescent peptide substrate for HIV-1 protease assay, *Opt. Mol. Probes Biomed. Appl.*, **6097** (2006), 1–12. <https://doi.org/10.1117/12.669174>
17. J. F. Lovell, J. Chen, M. T. Jarvi, W. Cao, A. D. Allen, Y. Liu, et al., FRET quenching of photosensitizer singlet oxygen generation, *J. Phys. Chem. B*, **113** (2009), 3203–3211. <https://doi.org/10.1021/jp810324v>
18. A. Hellebust, R. Richards-Kortum, Advances in molecular imaging: targeted optical contrast agents for cancer diagnostics, *Nanomedicine*, **7** (2012), 429–445. <https://doi.org/10.2217/nnm.12.12>
19. B. Fang, Y. Shen, B. Peng, H. Bai, L. Wang, J. Zhang, et al., Small-molecule quenchers for Förster resonance energy transfer: Structure, mechanism, and applications, *Angewandte Chemie*, **6** (2022). <https://doi.org/10.1002/anie.202207188>
20. Y. Wu, T. Jiang, Developments in FRET- and BRET-based biosensors, *Micromachines*, **13** (2022), 1789, <https://doi.org/10.3390/mi13101789>
21. Y. Zhang, H. Tang, W. Chen, J. Zhang, Nanomaterials used in fluorescence polarization based biosensors, *Int. J. Mol. Sci.*, **23** (2022), 8625, <https://doi.org/10.3390/ijms23158625>
22. S. M. A. El-atty, Health monitoring scheme-based FRET nanocommunications in internet of biological nanothings, *Nanomedicine*, **33** (2020), 1–17. <https://doi.org/10.1002/dac.4398>
23. O. Afzal, A. S. A. Altamimi, M. S. Nadeem, S. I. Alzarea, W. H. Almalki, A. Tariq, et al., Nanoparticles in drug delivery: From history to therapeutic applications, *Sci. Rep.*, **12** (2022). <https://doi.org/10.3390/nano12244494>
24. H. Pham, M. H. Soflaee, A. V. Karginov, L. W. Miller, Förster resonance energy transfer biosensors for fluorescence and time-gated luminescence analysis of rac1 activity, *Sci. Rep.*, **12** (2022). <https://doi.org/10.1038/s41598-022-09364-w>
25. M. Kuscü, A. Kiraz, O. B. Akan, Fluorescent molecules as transceiver nanoantennas: The first practical and high-rate information transfer over a nanoscale communication channel based on FRET, *Sci. Rep.*, **5** (2015). <https://doi.org/10.1038/srep07831>
26. S. Somathilaka, D. P. Martins, X. Li, Y. Li, S. Balasubramaniam, Inferring gene regulatory neural networks for bacterial decision making in biofilms, preprint, arXiv:2301.04225. <https://doi.org/10.48550/arXiv.2301.04225>
27. S. Do, C. Lee, T. Lee1, D. Kim, Y. Shin, Engineering DNA-based synthetic condensates with programmable material properties, compositions, and functionalities, *Sci. Adv.*, **8** (2022), 1–14. <https://doi.org/10.1126/sciadv.abj1771>

28. M. Swapna, U. M. Viswanadhula, R. Aluvalu, V. Varadarajan, K. Kotecha, Bio-signals in medical applications and challenges using artificial intelligence, *J. Sens. Actuator Netw*, **11** (2022), 1–18. <https://doi.org/10.3390/jsan11010017>
29. G. Leriche, G. Budin, Z. Darwich, D. Weltin, Y. Mély, A. S. Klymchenko, et al., A FRET-based probe with a chemically deactivatable quencher, *Chem. Commun.*, **48** (2012), 3224–3226. <https://doi.org/10.1039/C2CC17542H>
30. J. Zhang, L. Zhang, L. Chai, F. Yang, M. Du, T. Chen, Reliable measurement of the FRET sensitized-quenching transition factor for FRET quantification in living cells, *Micron*, **88** (2016), 7–15. <https://doi.org/10.1016/j.micron.2016.04.005>
31. J. R. Lakowicz, *Principles of Fluorescence Spectroscopy*, 3rd edition, Springer New York, NY (2006). <https://doi.org/10.1007/978-0-387-46312-4>
32. S. A. E. Marras, F. R. Kramer, S. Tyagi, Efficiencies of fluorescence resonance energy transfer and contact-mediated quenching in oligonucleotide probes, *Nucleic Acids Res.*, **30** (2002), 1–10. <https://doi.org/10.1093/nar/gnf121>
33. S. M. A. El-atty, R. Bider, S. El-Rabaie, MolCom system with Downlink/Uplink Biocyber Interface for Internet of Bio-NanoThings, *Int. J. Commun. Syst.*, **23** (2020), 1–21. <https://doi.org/10.1002/dac.4171>
34. U. A. K. Chude-Okonkwo, R. Malekian, B. T. Maharaj, Biologically inspired bio-cyber interface architecture and model for Internet of bio-nanotechnology applications, *IEEE Trans. Commun.*, **64** (2020), 3444–3455. <https://doi.org/10.1109/TCOMM.2016.2582870>
35. S. Mohamed, J. Dong, S. M. A. El-atty, M. A. Eissa, Bio-cyber interface parameter estimation with neural network for the Internet of Bio-Nano Things, *Wireless Pers. Commun.*, **123** (2022), 1245–1263. <https://doi.org/10.1007/s11277-021-09177-6>
36. A El-Fatyany, H. Wang, S. M. Abd El-atty, M. Khan, Biocyber interface-based privacy for Internet of Bio-nano Things, *Wireless Pers. Commun.*, **114** (2020), 1465–1483. <https://doi.org/10.1007/s11277-020-07433-9>
37. S. M. A. El-atty, N. A. Arafa, A. Abouelazm, O. Alfarraj, K. A. Lizos, F. Shawki, Performance analysis of an artificial intelligence nanosystem with biological Internet of NanoThings, *Comput. Mod. Eng. Sci.*, **133** (2022), 1–21. <https://doi.org/10.32604/cmes.2022.020793>
38. R. Bonnett, Photosensitizers of the porphyrin and phthalocyanine series for photodynamic therapy, *Chem. Soc. Rev.*, **24** (1995), 19–35. <https://doi.org/10.1039/CS99524FX001>
39. R. Kmiecik, K. Wojcik, P. Kulakowski, A. Jajszczyk, Signal generation and storage in FRET-based nanocommunications, *Nano Comm. Networks*, **21** (2019), 100254. <https://doi.org/10.48550/arXiv.1802.04886>
40. R. Pepperkok, A. Squire, S. Geley, P. I. H. Bastiaens, Simultaneous detection of multiple green fluorescent proteins in live cells by fluorescence lifetime imaging microscopy, *Curr. Biol.*, **9** (1999), 269–274. [https://doi.org/10.1016/s0960-9822\(99\)80117-1](https://doi.org/10.1016/s0960-9822(99)80117-1)



AIMS Press

©2023 the Author(s), licensee AIMS Press. This is an open access article distributed under the terms of the Creative Commons Attribution License (<http://creativecommons.org/licenses/by/4.0>)